PCCP

Effective π-electron number and Symmetry Perturbation Effect on the Two-photon Absorption of Oligofluorenes

Journal:	*Physical Chemistry Chemical Physics*
Manuscript ID	CP-ART-06-2021-002553.R2
Article Type:	Paper
Date Submitted by the Author:	27-Jul-2021
Complete List of Authors:	Abegão, Luis; Instituto de Física, Universidade Federal de Goiás Cocca, Leandro; Universidade de Sao Paulo Instituto de Fisica de Sao Carlos Mulatier, Jean-Christophe; Ecole Normale Supérieure de Lyon, Laboratoire de Chimie Pitrat, Delphine; Ecole Normale Supérieure de Lyon, Andraud, Chantal; Univ Lyon, Ens de Lyon, CNRS UMR5182, Université Lyon 1, Laboratoire de Chimie. Misoguti, Lino; USP, Physics Mendonca, Cleber R.; Univ Sao Paulo, FCM Vivas, Marcelo; Universidade Federal de Alfenas, Instituto de Ciência e Tecnologia Boni, Leonardo; Instituto de Física de Sâo Carlos - Universidade de Sâo Paulo, Física e Ciência dos Materiais

Effective π-electron number and Symmetry Perturbation Effect on the Two-photon Absorption of Oligofluorenes

Luis M. G. Abegão[a,b*], Leandro H. Z. Cocca[a], Jean-Christophe Mulatier[d], Delphine Pitrat[d], Chantal Andraud[d], Lino Misoguti[a], Cleber R. Mendonça[a], Marcelo G. Vivas[c] and Leonardo De Boni[a,*]

[a] Photonics Group, Instituto de Física de São Carlos, Universidade de São Paulo, CP 369, 13560-970 São Carlos, SP, Brazil

[b] Grupo de Fotônica, Instituto de Física, Universidade Federal de Goiás, 74690-900, Goiânia, GO, Brazil

[c] Laboratório de Espectroscopia Ótica e Fotônica, Universidade Federal de Alfenas, 37715-400 Pocos de Caldas, MG, Brazil

[d] Laboratoire de Chimie, Univ Lyon, Ens de Lyon, CNRS UMR 5182, , F69342 Lyon, France

* Author to whom correspondence should be addressed: luis.abegao@ufg.br, deboni@ifsc.usp.br

ABSTRACT

Fluorene-based molecules present significant nonlinear optical responses, multiphoton absorption in the visible, which, combined with the high fluorescence quantum yield in organic solvents, could make this class of materials potentially engaging in diverse photonics applications. Thus, herein, we have determined the two-photon absorption (2PA) of oligofluorenes containing three, five, and seven repetitive units by employing the wavelength-tunable femtosecond Z-scan technique. Our outcomes have shown that the 2PA cross-section in oligofluorenes presents an enhanced value of around 18 GM per N_{eff}, in which N_{eff} is the effective number of π-electrons, for the pure 2PA allowed transition (1^1A_g-like→2^1A_g-like). Furthermore, a weak 2PA transition was observed in the same spectral region strongly allowed by one-photon absorption (1^1A_g-like→1^1B_u-like). This last result suggests a molecular symmetry perturbation, probably induced by the molecular disorder triggered by the increase of moieties in the oligofluorene structure. We have calculated the permanent dipole moment difference related to the lowest-energy transition using the Lippert-Mataga formalism and the 2PA sum-over-states approach to confirm this assumption. Moreover, we have estimated the fundamental limits for the 2PA cross-section in oligofluorenes.

Keywords: oligofluorenes, fluorene, organic dyes, nonlinear optics, two-photon absorption.

1. INTRODUCTION

Organic photonics has been an emerging field in both pure and applied science due to the extensive synthesis investigation of organic compounds that pursue optimal optical, electrical, and chemical stability properties.[1-3] Among the enormous variety of organic molecular structures, aromatic polymers, at least the more stable ones, such as polyfluorenes, have become extremely popular for photonics applications. [4-6] For example, polyfluorenes derivatives can be used as 2PA photoinitiators (2PP) due to their high two-photon absorption (2PA) cross-section.[7] Still, they also can be employed to develop all-plastic, full-color, light-emitting diodes. [8-13]

Oligofluorenes and its derivatives have a high fluorescence quantum yield, thermal and photochemical stability combined with a large ground-, excited-state, and multiphoton absorption.[14-17] These features allied to the superior quality film formation make fluorene molecules excellent candidates for the fabrication of nonlinear optical devices. Although the oligofluorene's nonlinear optical response was widely studied in the past, the outcomes were achieved by using the nanosecond laser.[18-21] Therefore, there is a gap in the literature, regarding a complete 2PA spectral analysis of oligofluorenes, particularly by using femtosecond pulses. In oligofluorenes, the behavior of the 2PA spectral shape and its magnitude as a function of the effective number of electrons (N_{eff}) [22] could give the information of how much the polymeric chain needs to be increased to have a significant gain in the 2PA cross-section. That information should be gathered using ultra-short pulses (~ 160 fs) and low repetition rate (1 kHz) to avoid the contribution of thermal effects,[23] and excited-state absorption (stepwise 2PA),[24] which could mask the 2PA cross section final values.

Fortrie et. al.[25] proposed a molecular engineering route to achieve a strong 2PA cross-section and high transparency in the visible region for linear oligofluorenes.[26] In that work, they used nanosecond-pulses-induced fluorescence technique and observed that the 2PA oscillator strength per monomer linearly increases as a function of the increase of monomers. On the other hand, in the same paper, the author used an analytical three-energy excitonic model in order to interpret the found outcomes. According to this model, the 2PA oscillator strength per monomer tends to be constant for oligomers with monomer units higher than 2. Here, we have revisited such results by employing the wavelength-tunable femtosecond Z-scan technique.

Nonlinear optical phenomena are susceptible to molecular symmetry. For example, the second-order nonlinear optical response such as second-harmonic generation and hyper-Rayleigh scattering occurs only in noncentrosymmetric materials. Consequently, these nonlinear effects have been used as probes in several applications, including specific biomolecular interactions.[27] In the same context, for 2PA, no such symmetry constraints exist: in centrosymmetric molecules, the electric-dipole selection rules for optical transitions have different parities: *gerade-ungerade* or vice-versa for one-photon and *gerade-gerade* or *ungerade-ungerade* for 2PA. [28, 29] Although the Fluorene molecule did not present an inversion center, it has a plane symmetry, leading to the electric-dipole selection rules. [30] Therefore, the fluorene molecule belongs to the well-defined symmetry point group C_{2v}.[31] According to the spectroscopic notation, the fluorene molecule has the ground-state 1^1A_g, the first one-photon allowed excited state with symmetry 1^1B_u and the second excited state of symmetry 2^1A_g strongly allowed by 2PA.[15, 30, 32] Some works have shown the intrinsic symmetry breaking perturbation in molecular systems or induced by interaction with solvent, electric field, temperature, and so on.[33-36] However, to the best of our knowledge, the symmetry perturbation effect

on the 2PA properties of unsubstituted and linear oligofluorenes has not been reported yet.

Herein, we performed an extensive optical study taken into account linear absorption (1PA), fluorescence spectroscopy, solvatochromism as input data to help investigate and describe the 2PA spectral shape and its σ_{2PA} magnitude as a function of the N_{eff} of the linear and unsubstituted oligofluorenes, designated by trifluorene, pentafluorene, and heptafluorene. The wavelength-tunable femtosecond Z-scan technique was employed to measure the 2PA cross-section spectrum for these molecules. In addition, the sum-over-states (SOS) approach was used to improve the 2PA analysis.

2. MATERIALS AND METHODS

2.1 COMPOUNDS

The trifluorene and pentafluorene have been synthesized following the procedure developed by Anémian et. al.[17], while the hepatafluorene was obtained according to Ref. [37]. The molecular structures are shown in Figure 1. The three distinct oligofluorenes compounds are composed of three, five, and seven single fluorene moieties.

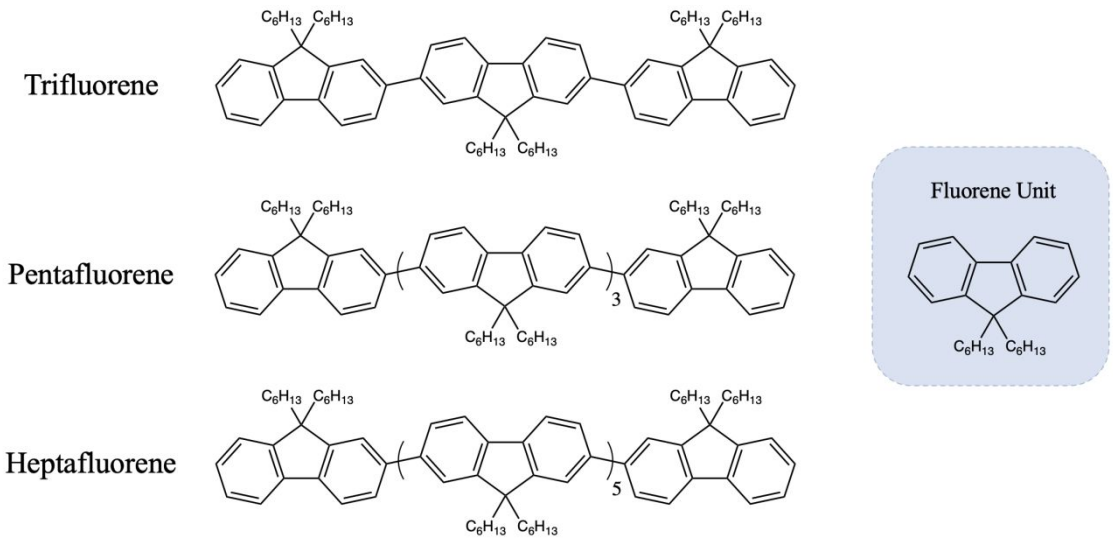

Figure 1: Molecular structures of the linear and unsubstituted oligofluorenes investigated in this work.

2.2 LINEAR OPTICAL MEASUREMENTS

The trifluorene, pentafluorene, and heptafluorene molecules were dissolved in toluene at low concentrations: 5.5×10^{-6} M, 4.5×10^{-6} M, and 1.5×10^{-6} M, respectively. A commercial Shimadzu UV-Vis 1800 spectrophotometer was employed to determine the one-photon absorption (1PA) bands. Besides that, a commercial F-7000 Hitachi fluorescence spectrophotometer was used to determine the steady-state fluorescence. All linear optical measurements were recorded using 10-mm optical path quartz cuvettes. A detailed description regarding the equations and methods used with the linear optical measurements can be found in sections 1.1, 1.2, and 1.3 in the supplementary information (SI).

2.3 NONLINEAR OPTICAL MEASUREMENT

An optical parametric amplifier (OPA, Topas, Light Conversion) pumped by a pulse of 775 nm delivered by a Ti:Sapphire chirped-pulse amplifier laser system (CPA 2001, Clark MXR) was used in the open-aperture Z-Scan technique [38] to measure the 2PA spectra in the spectral range of 470-800 nm.

The 2PA cross-section spectra ($\sigma_{2PA}(\lambda)$) were determined at a higher concentration (~10^{-2} – 10^{-3} M) compared with the linear optical measurements and a 2-mm optical path quartz cuvette was used instead of the 10-mm. The trifluorene, pentafluorene, and heptafluorene concentrations were 6.0×10^{-3}M, 1.3×10^{-2} M, and 9.4×10^{-3} M, respectively. More details about the Z-scan data analysis can be found in section 1.4 from the SI.

3. QUANTUM CHEMICAL CALCULATIONS

The Gaussian 16 program package [39] was used to estimate the molecular cavity volume of all studied molecules in the toluene medium. The CAM-B3LYP/6-311++G(2d,p)[40] level of theory was used first to optimize the geometry and second to calculate the volume in toluene solvent medium employing a polarizable continuum model (PCM), using the integral equation formalism variant (IEF-PCM).[41] The optimized geometries in cartesian coordinates are presented in Tables S1 and S2 in the SI. The surface type used to represent the solute-solvent boundary was the solvent excluding surface (SES).[42] Also, we have calculated the cavity volume considering the Onsager-model (OM).[43] Henceforth, the cavity volumes will be described as vol_{SES} and vol_{OM} as the estimated volume obtained for all molecules, via SES and OM approaches, respectively. Both volumes are shown in Table 1 and were used as an input parameter to calculate the permanent electric dipole moment between the ground and the first excited state.

4. RESULTS AND DISCUSSION

Figure 2 exhibits the ground-state absorption and fluorescence spectra of the three studied molecules. It is possible to observe that all molecules present 1PA bands in the ultra-violet (UV) region, in a range that covers 300 – 400 nm. Besides that, the three molecules present fluorescence emission in the UV-visible region, in a spectral range from 370 – 525 nm containing a vibrational progression for all molecules. Trifluorene, pentafluorene and heptafluorene present molar absorptivity peaks of 5.8×10^4 $M^{-1}cm^{-1}$ at 350 nm, 8.6×10^4 $M^{-1}cm^{-1}$ at 360 nm, and 16.3×10^4 $M^{-1}cm^{-1}$ at 370 nm, respectively. It is noted that the molar absorptivity peak increase 1.5 times considering the trifluorene and pentafluorene molecules $\left(\frac{\varepsilon_{penta}}{\varepsilon_{tri}} = 1.5\right)$ and increase 1.9

157 times considering the pentafluorene and heptafluorene molecules $\left(\frac{\varepsilon_{hepta}}{\varepsilon_{penta}} = 1.9\right)$.

158 Moreover, it is also possible to observe that the increase of the monomer units (fluorene
159 moieties) in the investigated oligomers creates a bathochromic shift in the spectral
160 position of the absorption band maxima, i.e., the trifluorene has its maximum at 350 nm
161 (3.54 eV), pentafluorene at 360 nm (3.44 eV), and heptafluorene at 370 nm (3.35 eV),
162 as previously observed in Ref. [17]. Such behavior can be explained by considering the
163 increase of π-electrons.

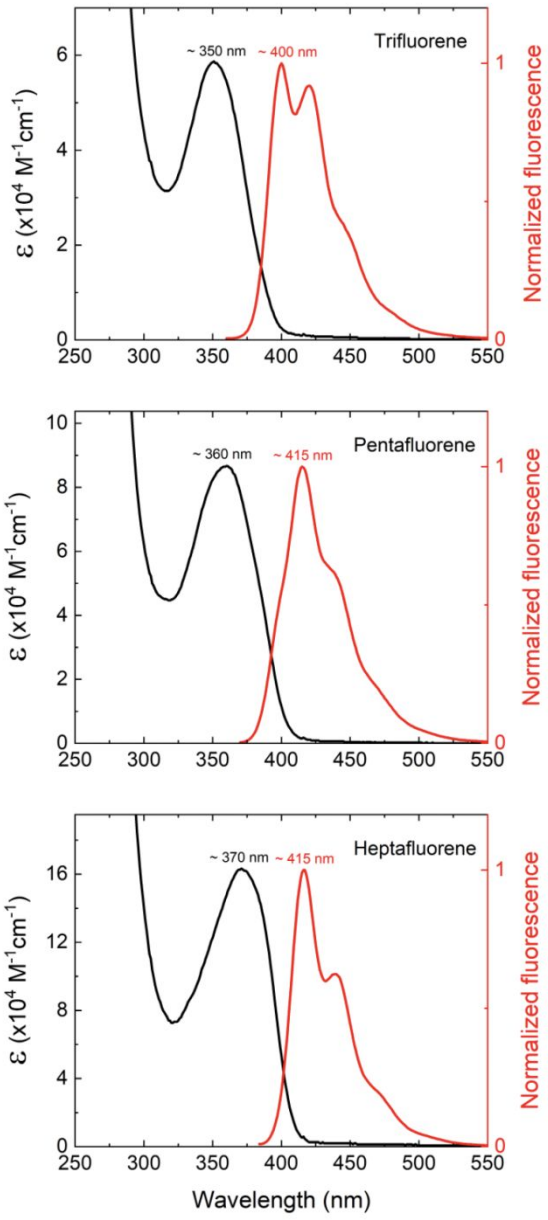

164

Figure 2: Molar absorptivity (black lines) and fluorescence spectra (red lines) of the oligofluorenes studied in this work (trifluorene, pentafluorene and heptaflurene).

The energies corresponding to these wavelengths are the energies with a higher probability to promote an electronic transition from the ground-state (1^1A_g) to the first excited state (1^1B_u). [32] A transition 1^1A_g-like→1^1B_u-like can be quantified by evaluating the transition dipole moment μ_{01}, expressed in Debye units. The μ_{01} evaluation of the three oligofluorenes was obtained in the SI, and the results are $8.5 \pm 0.9\, D$ for trifluorene, $11.3 \pm 1.1\, D$ for pentafluorene, and $14.1 \pm 1.4\, D$ for heptafluorene. It is observed that μ_{01} increases 1.33 times considering pentafluorene and trifluorene molecules; μ_{01} increases 1.25 times considering heptafluorene and pentafluorene molecules. In this way, it is possible to say that the molecules exhibit a very similar increase rate considering the μ_{01} values, or in other words, $\frac{\mu_{01_{penta}}}{\mu_{01_{tri}}} \cong \frac{\mu_{01_{hepta}}}{\mu_{01_{penta}}}$.

The effective number of electrons (N_{eff}) of any oligomer is an important parameter, in particular, if it will be used to normalize some spectroscopic parameters, such as μ_{01}, $\Delta\mu_{01}$, and σ_{2PA}. This parameter can be calculated using Eq. 1, [22] in which n_i is the number of π-electrons of each π-conjugated part of the molecule.

$$N_{eff} = \sqrt{\sum_i {n_i}^2} \qquad (1).$$

In this particular study, each monomer, i.e., the single fluorene moiety, has 12 π-electrons. Thus, calculating N_{eff}, the trifluorene presents $N_{eff} = \sqrt{3x12^2} = 20.78$, the pentafluorene presents $N_{eff} = \sqrt{5x12^2} = 26.80$, and the heptafluorene presents $N_{eff} = \sqrt{7x12^2} = 31.74$. Considering the values of μ_{01} as well as the N_{eff} of each molecular structure, it is possible to see that there is a contribution of about 0.4 D per N_{eff} ($\frac{\mu_{01_{tri}}}{N_{eff_{tri}}} = 0.40$, $\frac{\mu_{01_{penta}}}{N_{eff_{penta}}} = 0.42$, and $\frac{\mu_{01_{hepta}}}{N_{eff_{hepta}}} = 0.44$).

The results of solvatochromic measurements and the linear fittings obtained through the Lippert-Mataga equation, aiming the $\Delta\mu_{01}$ determination, are exhibited in the SI (section 1). The $\Delta\mu_{01}$ values for trifluorene, pentafluorene, and heptafluorene were estimated by using two-cavity volumes (vol_{SES} and vol_{OM}): $\Delta\mu_{01}^{SES}$ and $\Delta\mu_{01}^{OM}$. As shown in Table 1, the $\Delta\mu_{01}$ values, for all compounds, calculated by using two different cavity volumes revealed a difference of around 30%, still inside the margin of error associated to the $\Delta\mu_{01}$. From the theoretical point of view, the fluorene has a symmetry plane and, therefore, the difference between the static dipole moment from the first excited and ground state is minimal (Δμ=0.29 D). However, our outcomes show that $\Delta\mu_{01}$, regardless of being estimated using SSE or OM cavity approaches, is considerably higher for the oligofluorenes than the fluorene molecule and, more important, such molecular parameter increases as a function of the increase of N_{eff}. This result indicates that we have molecular conformations in solution with different symmetry levels due to the increase of fluorene moieties. Indeed, symmetrical fluorene molecules with strong electronic-vibrational coupling present a double-minimum excited state energy surface, i.e., symmetrical and unsymmetrical electronic distribution. [14, 44] In this case, the unsymmetrical electronic distribution generates a higher $\Delta\mu_{01}$ value. Aiming at a better comparison between the determined linear optical parameters of each studied molecule, Table 1 shows the values of μ_{01}, $\Delta\mu_{01}^{OM}$, vol_{OM}, $\Delta\mu_{01}^{SES}$, vol_{OM}, $\Delta\mu_{01}^{OM}$, and dv/dF (Solvatochromic Stokes shift, which can be found in SI).

Table1: Spectroscopic parameters obtained by 1PA and QCC[(i)] for trifluorene, pentafluorene and heptafluorene molecules.

	$\boldsymbol{\mu_{01}\,(D)}$	$\boldsymbol{\Delta\mu_{01}^{OM}(D)}$	$\boldsymbol{vol_{OM}\,(\dot{A}^3)^{(i)}}$	$\boldsymbol{\Delta\mu_{01}^{SES}(D)}$	$\boldsymbol{vol_{SSE}\,(\dot{A}^3)^{(i)}}$	$\boldsymbol{\frac{dv}{dF}(cm^{-1})}$
Trifluorene	8.5 ± 0.9	3.5 ± 1.1	1032.5	2.9 ± 0.9	682.6	-252 ± 191
Pentafluorene	11.3 ± 1.1	4.5 ± 1.3	1570.0	3.9 ± 1.1	1113.1	-275 ± 186
Heptafluorene	14.1 ± 1.4	5.8 ± 1.6	2447.4	4.6 ± 1.3	1554.1	-286 ± 180

210

211 The open-aperture Z-scan technique was used to obtain the 2PA as a function of
212 the excitation wavelength (470-800 nm). Figure 3 presents the 2PA spectra (black
213 circles) for trifluorene, pentafluorene, and heptafluorene.

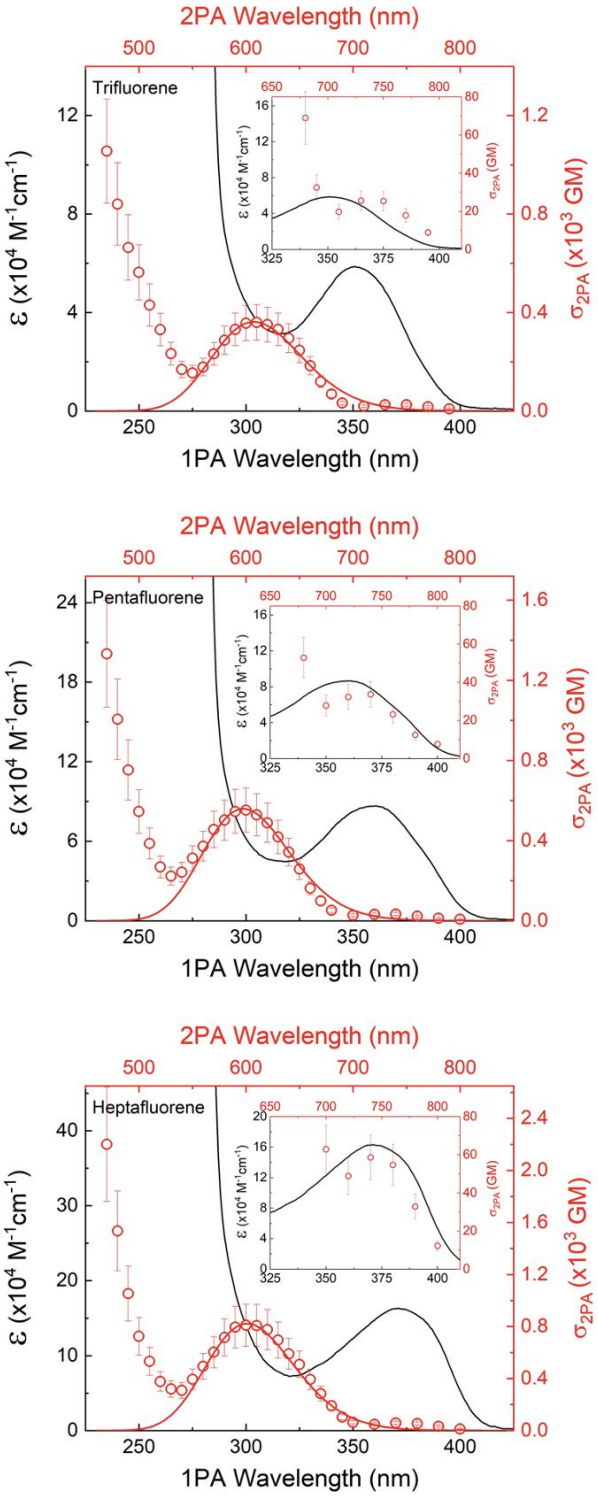

214

Figure 3: Molar absorptivity (black lines) and 2PA cross section (red circles) fitted by the SOS method (red lines).

It is observed that all molecules show two 2PA bands in a visible-IR spectral region. The highest energy 2PA band is localized in a spectral range from 520-700 nm for all samples, where the maximum σ_{2PA} magnitude can be found approximately at 610 nm for all molecules. As expected, the highest σ_{2PA} is found for the heptafluorene (~ 810 GM), while the pentafluorene presents a σ_{2PA} value of 550 GM, and the lowest σ_{2PA} value of *c.a.* 360 GM is obtained for the trifluorene. The efficient 2PA cross-section in this wavelength range evaluated for every compound can be attributed to the high electronic delocalization at the excited state of fluorene-based molecules.[11, 45] This transition can reach thousands of GM in oligofluorenes[18, 25] and poly(fluorene) derivatives.[46-49] Interesting to say that the σ_{2PA} peak for poly(fluorene) derivatives occurs at the same energy value as those observed in oligofluorenes (monomers units higher than 2), which is *c.a.* 2.03 eV (~ 610 nm). These results suggest that the nature of the higher-energy 2PA transition is intrinsically related to the fluorene molecular structure. On the other hand, in the NIR spectral region (~700-800 nm), a weak 2PA band is noticed, as one could check in the inset of Figure 3. Such transition has never been experimentally observed previously for these molecules. This 2PA band seems to be centered between 700-740 nm, approximately half of the energy needed to reach the lowest-energy 1PA allowed band, corresponding to the $1A_g$-like $\rightarrow 1B_u$-like transition. Herein, the bathochromic shift obtained for the 2PA spectra was analogous to those observed in the one-photon absorption spectra. The σ_{2PA} magnitude recorded for this lower energy transition (25-59 GM) is one order of magnitude lower than its higher energy analog. The existence of this band confirms the symmetry perturbation, [50] corroborating the data from the Lippert-Mataga equation. In general, but not as a rule, slight distortion in the molecular structure of the chromophore caused by solvent,

electric field, temperature, and so on can generate symmetry perturbation that contributes to the lowest-energy 2PA band weak intensity. [33, 34] Finally, all molecules exhibit the intermediate state resonance enhancement effect in the 2PA transitions for wavelengths lower than 520 nm. Such effect occurs as the excitation photon energy approaches from the first one-photon allowed excited state and its magnitude depending on the several molecular parameters. [51]

Take into account only the higher-energy 2PA band, the trifluorene, pentafluorene, and heptafluorene molecules present maximum σ_{2PA} at ~610 nm with a value of 360 GM, 552 GM, and 810 GM, respectively. For the 2PA cross-section related to the higher-energy transition, it is noted that there is an increase in σ_{2PA} of about 1.5 times considering pentafluorene and trifluorene molecules ($\frac{\sigma_{2PA}(610\ nm)_{penta}}{\sigma_{2PA}(610\ nm)_{tri}} = 1.53$), in the same way, there is an increase in the $\sigma_{2PA}(610\ nm)$ of about 1.5 times considering heptafluorene and pentafluorene molecules ($\frac{\sigma_{2PA}(610\ nm)_{hepta}}{\sigma_{2PA}(610\ nm)_{penta}} = 1.47$). Performing a parallel between the molecules $\sigma_{2PA}(610\ nm)$ values and the N_{eff} of each molecule, It is observed that $\frac{\sigma_{2PA}(610\ nm)_{tri}}{N_{eff_{tri}}} = 17.3\ GM$, $\frac{\sigma_{2PA}(610\ nm)_{penta}}{N_{eff_{penta}}} = 18.3\ GM$ and $\frac{\sigma_{2PA}(610\ nm)_{hepta}}{N_{eff_{hepta}}} = 20.2\ GM$. Here, we have normalized concerning the trifluorene molecule the resonance enhancement effect, which strongly contributes to the higher-energy 2PA transition, as will be shown later. Thus, taking into account the experimental error (around 20%) there is a contribution of about 18 GM per N_{eff} in σ_{2PA} for the higher-energy 2PA transition. In fact, our outcomes show that the 2PA cross-section per monomer (for example) is almost constant as a function of the increase of monomers number in accordance with the three-energy excitonic model described in Ref. [25].

As shown, the 1PA and 2PA allowed transition for the unsubstituted and linear fluorene molecules are related only to the energy levels; 1^1A_g-like (ground-state), 1^1B_u-

like (strongly 1PA allowed), and 2^1A_g-like (strongly 2PA allowed). In this case, to shed more light on the description of the σ_{2PA}, we can employ the SOS approach considering a few energy levels. For the higher-energy 2PA band, we can consider a three-level energy system that consists of the ground-state (1^1A_g-like), one intermediate 1PA allowed excited state (1^1B_u-like), and the 2PA allowed final excited state (2^1A_g-like). Thus, the σ_{2PA} assuming linearly polarized light and that the dipole moments are parallel as:

$$\sigma_{0\to 2}^{(2PA)}(\omega) = \frac{2\,(2\pi)^5}{5(nhc)^2} L^4\, R(\omega)\, |\vec{\mu}_{01}|^2\, |\vec{\mu}_{12}|^2\, g_{02}(2\omega) \qquad (2)$$

in which ω and ω_{01} are the excitation laser and first electronic transition frequencies, $|\vec{\mu}_{01}|^2$ is the transition dipole moment between the excited states $|1B_u\rangle \to |2A_g\rangle$, and $R(\omega,\omega_{01}) = {\omega^2}/{(\omega_{01}-\omega)^2 + \Gamma_{01}^2(\omega)}$ is the resonance enhancement factor. Γ is the full-width at half maximum considering the Gaussian line-shaped. This parameter can be determined from the lowest-energy absorption band (Figure 2). We have found $R(610\,nm,350\,nm) = 1.63$ for trifluorene, $R(610\,nm,360\,nm) = 1.83$ for pentafluorene and $R(610\,nm,370\,nm) = 2.05$ for heptafluorene. Eq. 2 describes the σ_{2PA} for noncentrosymmetric molecules, in which the lowest-energy 2PA transition is much weaker than the higher-energy transition. In this case, the factor $\frac{|\vec{\mu}_{01}||\vec{\mu}_{12}|}{(\omega_{01}-\omega)+i\Gamma} \gg \frac{|\vec{\mu}_{02}||\Delta\vec{\mu}_{02}|}{\omega}$ dominates the 2PA allowed transition.[52] The red line in Fig. 3 illustrates the 2PA fitting using Eq. 2, while Table 2 gathered the spectroscopic data. The only adjust parameter in Eq. 2 is the $|\vec{\mu}_{12}|$ that describes the amplitude of the 2PA band. All the other parameters can be obtained from the 1PA spectrum. The high $|\vec{\mu}_{12}|$ values obtained are in accordance with the large excited-state absorption reported for the fluorene-based molecules reported in Refs. [46, 53, 54]. It is also observed that, contrary to

all-optical determined parameters, $|\vec{\mu}_{12}|$ presents a decrease according to the fluorene moiety insertion. Such behavior can be explained because the increase of moieties favors the lowest-energy 2PA transition in detriment to the higher-energy 2PA transition due to the disturbance of molecular symmetry, as pointed out by the solvatochromic measurements. In general, strongly 2PA allowed transitions are weakly allowed by 1PA and vice-versa.[34]

In this same context, we have assumed a two-energy level system for the lowest energy 2PA band located at 700-800 nm (1^1A_g-like $\rightarrow 1^1B_u$-like). In this case, we can use the 2PA spectroscopy as a robust technique to measure the permanent dipole moment change ($|\Delta\vec{\mu}_{01}|$) and molecular structure in randomly oriented molecules as in a solution.[34, 55] Thus, the permanent dipole moment difference can be evaluated through the lowest-energy 2PA transition by using:

$$|\Delta\vec{\mu}_{01}| = \left(\frac{5}{2(2\pi)^3 3 \times 10^3 \ln(10) L^2} \frac{N_A hc}{\epsilon_{max}(\omega_{01})} \frac{n}{\omega_{01}} \sigma_{0\rightarrow 1}^{(2PA)}(\omega_{01})\right)^{\frac{1}{2}} \quad (3).$$

It is important to note that we removed the higher-energy 2PA band contribution for the 2PA cross-section of the 1^1A_g-like $\rightarrow 1^1B_u$-like transition. Figure 4 exhibits the values $\Delta\mu_{01}$ determined via the Lippert-Mataga equation and 2PA-SOS method. As seen, that is a good agreement between these methods corroborating the disturbance of molecular symmetry for the fluorene molecules containing three or more repetitive units.

Oligofluorenes present an effective conjugation length of approximately 12 repetitive units in good solvents with one-photon resonance at ~400 nm. [56] Thus, it is expected that the saturation of the 2PA cross-section occurs at ~2200 GM for the strongly 2PA allowed band. To estimate such value, we considered the correction in the resonance enhancement factor ($R(610\ nm, 400\ nm) = 2.84$).

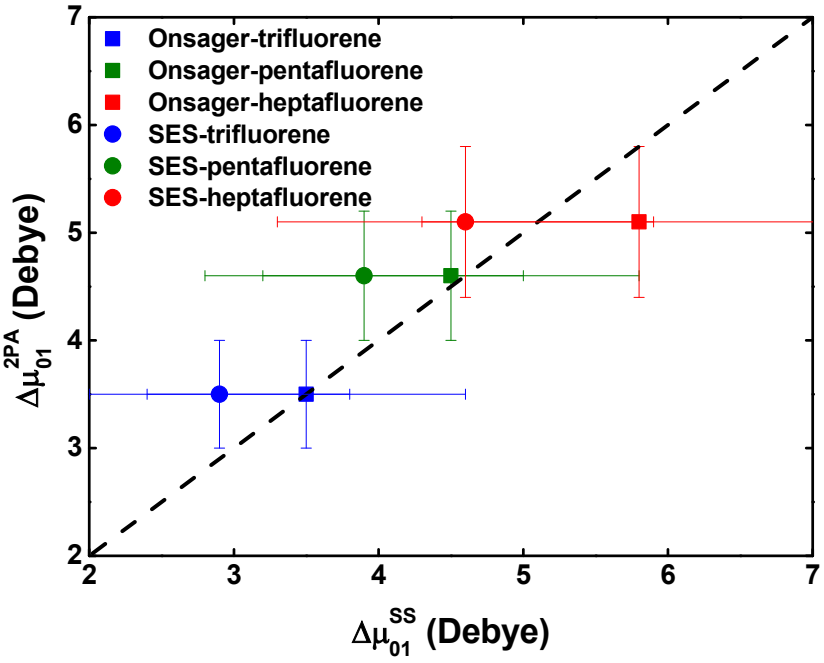

Figure 4 – Comparison between the $\Delta\mu_{01}$ values obtained from the Lippert-Mataga equation (bottom-axis) and 2PA-SOS method (left-axis) for the trifluorene (blue symbols), pentafluorene (green symbols), and the heptafluorene (red symbols). The squared symbols are the results obtained using the cavity volume obtained via SES, while the circled symbols depict the results obtained by OM cavity type. The dashed line shows the perfect correspondence.

Table 2: Spectroscopic parameters obtained by 2PA for trifluorene, pentafluorene, and heptafluorene molecules. Standard deviation for the 2PA cross section is 20 %.

	S_{ij}^{2PA} $[nm]$	σ^{2PA} (GM)	$\Delta\mu_{01}(D)$	μ_{12} (D)
Trifluorene	S_{02} [610]	360	-	19.0 ± 2.0
	S_{01} [700]	25	3.5 ± 0.5	-
Pentafluorene	S_{02} [610]	552	-	16.5 ± 2.0
	S_{01} [720]	34	4.6 ± 0.6	-
Heptafluorene	S_{02} [610]	810	-	15.1 ± 2.5
	S_{01} [740]	59	5.1 ± 0.7	-

5. CONCLUSIONS

We have shown that oligofluorene has a high 2PA ratio as a function of the effective π-electron of ~18 GM per N_{eff} for the pure 2PA transition (1^1A_g-like $\rightarrow 2^1A_g$-like). Such a large 2PA ratio is associated with the strong intramolecular interaction between the fluorene units, leading to the remarkable excited state absorption that reflects the high values for the transition dipole moment between the excited state 1^1B_u-like and 2^1A_g-like. Our finding also indicates that the increase of the repetitive units in the fluorene structure contributes to the molecular symmetry perturbation. Consequently, the strongly 1PA allowed transition (1^1A_g-like$\rightarrow 1^1B_u$-like) became allowed by 2PA. A possible explanation for the symmetry disturbance is related to the slight rotation angle between the fluorene moieties in solution, which can confer a quadrupolar character for the oligofluorenes. Thus, the electronic-vibrational coupling combined with the small quadrupolar moment may generate a double-minimum excited state energy surface as reported in Ref.[14, 44] for fluorene derivatives. Finally, the results allowed estimating the fundamental limit of the 2PA cross-section for oligofluorene of ~2200 GM.

Supporting Information

The first section includes the experimental results, such as the Gaussian decomposition of the absorption bands, solvatochromism measurements, and Z-scan signatures (obtained by femtosecond pulses). Section two exhibits the optimized geometries used to achieve the cubic radius by using the Gaussian program package.

V Acknowledgments

Financial support from FAPESP (Fundação de Amparo à Pesquisa do Estado de São Paulo, grants 2011/12399-0, 2015/20032-0 2016/20886-1 and 2018/11283-7),

FAPEMIG (Fundação de Amparo à Pesquisa do Estado de Minas Gerais, grant APQ-01469-18), CNPq (Conselho Nacional de Desenvolvimento Científico e Tecnológico, grant 425180/2018-2), Coordenação de Aperfeiçoamento de Pessoal de Nível Superior (CAPES) Finance Code 001, Army Research Laboratory (W911NF-17-1-0123) and Air Force Office of Scientific Research (FA9550-12-1-0028) are acknowledged. We thank the computer support from LaMCAD/UFG (Laboratório Multiusuário de Computação de Alto Desempenho/Universidade Federal de Goiás).

References

1. H. S. Nalwa and S. Miyata, *Nonlinear Optics of Organic Molecules and Polymers*, CRC Press 1996.

2. M. G. Vivas, D. L. Silva, J. Malinge, M. Boujtita, R. Zalesny, W. Bartkowiak, H. Agren, S. Canuto, L. De Boni, E. Ishow and C. R. Mendonca, *Sci. Rep.*, 2014, **4**.

3. E. Collini, *Phys. Chem. Chem. Phys.*, 2012, **14**, 3725-3736.

4. G. Tsiminis, A. Ruseckas, I. D. W. Samuel and G. A. Turnbull, *Appl. Phys. Lett.*, 2009, **94**.

5. J. Moughames, S. Jradi, T. M. Chan, S. Akil, Y. Battie, A. E. Naciri, Z. Herro, S. Guenneau, S. Enoch, L. Joly, J. Cousin and A. Bruyant, *Sci. Rep.*, 2016, **6**.

6. B. Mettra, F. Appaix, J. Olesiak-Banska, T. Le Bahers, A. Leung, K. Matczyszyn, M. Samoc, B. van der Sanden, C. Monnereau and C. Andraud, *ACS Appl. Mater. Inter.*, 2016, **8**, 17047-17059.

7. I. Fitilis, M. Fakis, I. Polyzosa, V. Giannetas and P. Persephonis, *J. Photochem. Photobio. A: Chem.*, 2010, **215**, 25-30.

8. J. H. Burroughes, D. D. C. Bradley, A. R. Brown, R. N. Marks, K. Mackay, R. H. Friend, P. L. Burn and A. B. Holmes, *Nature*, 1990, **347**, 539-541.

9. B. H. Cumpston, S. P. Ananthavel, S. Barlow, D. L. Dyer, J. E. Ehrlich, L. L. Erskine, A. A. Heikal, S. M. Kuebler, I. Y. S. Lee, D. McCord-Maughon, J. Q. Qin, H. Rockel, M. Rumi, X. L. Wu, S. R. Marder and J. W. Perry, *Nature*, 1999, **398**, 51-54.

10. R. H. Friend, R. W. Gymer, A. B. Holmes, J. H. Burroughes, R. N. Marks, C. Taliani, D. D. C. Bradley, D. A. Dos Santos, J. L. Bredas, M. Logdlund and W. R. Salaneck, *Nature*, 1999, **397**, 121-128.

11. E. Y. Choi, L. Mazur, L. Mager, M. Gwon, D. Pitrat, J. C. Mulatier, C. Monnereau, A. Fort, A. J. Attias, K. Dorkenoo, J. E. Kwon, Y. Xiao, K. Matczyszyn, M. Samoc, D. W. Kim, A. Nakao, B. Heinrich, D. Hashizume, M. Uchiyama, S. Y. Park, F. Mathevet, T. Aoyama, C. Andraud, J. W. Wu, A. Barsella and J. C. Ribierre, *Phys. Chem. Chem. Phys.*, 2014, **16**, 16941-16956.

12. D. Das, P. Gopikrishna, A. Singh, A. Dey and P. K. Iyer, *Phys. Chem. Chem. Phys.*, 2016, **18**, 7389-7394.

13. S. J. Li, Z. Q. Li, C. Y. Liu, X. Y. Zhang, Z. H. Zhang, W. B. Guo, L. Shen, S. P. Ruan and L. Zhang, *Phys. Chem. Chem. Phys.*, 2017, **19**, 15207-15214.

14. K. D. Belfield, M. V. Bondar, C. O. Yanez, F. E. Hernandez and O. V. Przhonska, *J. Mater. Chem.*, 2009, **19**, 7498-7502.

15. K. D. Belfield, A. R. Morales, B. S. Kang, J. M. Hales, D. J. Hagan, E. W. Van Stryland, V. M. Chapela and J. Percino, *Chem. Mater.*, 2004, **16**, 4634-4641.

16. K. D. Belfield, X. B. Ren, E. W. Van Stryland, D. J. Hagan, V. Dubikovsky and E. J. Miesak, *J. Am. Chem. Soc.*, 2000, **122**, 1217-1218.

17. R. Anemian, J. C. Mulatier, C. Andraud, O. Stephan and J. C. Vial, *Chem. Commun.*, 2002, 1608-1609.

18. R. Anemian, J. C. Mulatier, C. Andraud, Y. Morel, O. Stephan and P. L. Baldeck, in *Multiphoton Absorption and Nonlinear Transmission Processes:*

Materials, Theory, and Applications, eds. K. D. Belfield, S. J. Caracci, F. Kajzar, C. M. Lawson and A. T. Yeates 2003, vol. 4797, pp. 25-32.

19. C. Barsu, C. Andraud, N. Amari, S. Spagnoli and P. L. Baldeck, *J. Nonl. Opt. Phys. Mater.*, 2005, **14**, 311-318.

20. C. Barsu, R. Anemian, C. Andraud, O. Stephan and P. L. Baldeck, *Mol. Crys. Liq. Cryst.*, 2006, **446**, 175-182.

21. Y. Morel, A. Irimia, P. Najechalski, Y. Kervella, O. Stephan, P. L. Baldeck and C. Andraud, *J. Chem. Phys.*, 2001, **114**, 5391-5396.

22. M. G. Kuzyk, *J. Chem. Phys.*, 2003, **119**, 8327-8334.

23. M. L. Miguez, T. G. B. De Souza, E. C. Barbano, S. C. Zilio and L. Misoguti, *Opt. Exp.*, 2017, **25**, 3553-3565.

24. K. Teuchner, J. Ehlert, W. Freyer, D. Leupold, P. Altmeyer, M. Stucker and K. Hoffmann, *J. Fluoresc.*, 2000, **10**, 275-281.

25. R. Fortrie, R. Anemian, O. Stephan, J. C. Mulatier, P. L. Baldeck, C. Andraud and H. Chermette, *J. Phys. Chem. C*, 2007, **111**, 2270-2279.

26. C. Andraud, R. Fortrie, C. Barsu, O. Stephan, H. Chermette and P. L. Baldeck, in *Photoresponsive Polymers Ii*, eds. S. R. Marder and K. S. Lee 2008, vol. 214, pp. 149-203.

27. P. C. Ray and P. K. Das, *Chem. Phys. Lett.*, 1997, **281**, 243-246.

28. K. D. Bonin and T. J. McIlrath, *J.Opt. Soc. Am. B*, 1984, **1** 52-55

29. W. M. McClain, *J. Chem. Phys.*, 1971, **55**, 2789-2796.

30. S. Zein, F. Delbecq and D. Simonb, *Phys. Chem. Chem. Phys.*, 2008, **11**, 694–702.

31. S. Chakrabortya, P. Das, S. Manogaranb and P. K. Das, *Vib. Spectrosc.*, 2013, **68**, 162-169.

32. P. Najechalski, Y. Morel, O. Stephan and P. L. Baldeck, *Chem. Phys. Lett.*, 2001, **343**, 44-48.

33. M. G. Vivas, L. De Boni, T. M. Cooper and C. R. Mendonca, *ACS Photon.*, 2014, **1**, 106-113.

34. A. Rebane, M. Drobizhev, N. S. Makarov, G. Wicks, P. Wnuk, Y. Stepanenko, J. E. Haley, D. M. Krein, J. L. Fore, A. R. Burke, J. E. Slagle, D. G. McLean and T. M. Cooper, *J. Phys. Chem. A*, 2014, **118**, 3749-3759.

35. K. Bhattacharyya, A. Surendran, C. Chowdhury and A. Datta, *Phys. Chem. Chem. Phys.*, 2016, **18**, 31160-31167.

36. T. Gallavardin, C. Armagnat, O. Maury, P. L. Baldeck, M. Lindgren, C. Monnereau and C. Andraud, *Chem. Commun.*, 2012, **48**, 1689-1691.

37. W. Y. Lai, X. R. Zhu, Q. Y. He and W. Huang, *Chem. Lett.*, 2009, **38**, 392-393.

38. M. Sheikbahae, A. A. Said, T. H. Wei, D. J. Hagan and E. W. Vanstryland, *IEEE J. Quant. Elect.*, 1990, **26**, 760-769.

39. G. W. T. M. J. Frisch, H. B. Schlegel, G. E. Scuseria, M. A. Robb, J. R. Cheeseman, G. Scalmani, V. Barone, G. A. Petersson, H. Nakatsuji, X. Li, M. Caricato, A. V. Marenich, J. Bloino, B. G. Janesko, R. Gomperts, B. Mennucci, H. P. Hratchian, J. V. Ortiz, A. F. Izmaylov, J. L. Sonnenberg, D. Williams-Young, F. Ding, F. Lipparini, F. Egidi, J. Goings, B. Peng, A. Petrone, T. Henderson, D. Ranasinghe, V. G. Zakrzewski, J. Gao, N. Rega, G. Zheng, W. Liang, M. Hada, M. Ehara, K. Toyota, R. Fukuda, J. Hasegawa, M. Ishida, T. Nakajima, Y. Honda, O. Kitao, H. Nakai, T. Vreven, K. Throssell, J. A. Montgomery, Jr., J. E. Peralta, F. Ogliaro, M. J. Bearpark, J. J. Heyd, E. N. Brothers, K. N. Kudin, V. N. Staroverov, T. A. Keith, R. Kobayashi, J. Normand, K. Raghavachari, A. P. Rendell, J. C. Burant, S. S. Iyengar, J. Tomasi, M. Cossi, J. M. Millam, M. Klene, C. Adamo, R. Cammi, J. W. Ochterski, R. L. Martin, K. Morokuma, O. Farkas, J. B. Foresman, and D. J. Fox, , Gaussian, Inc., Wallingford CT, Revision C.01 edn., 2016.

40. T. Yanai, D. P. Tew and N. C. Handy, *Chem. Phys. Lett.*, 2004, **393**, 51-57.

448 41. J. Tomasi, B. Mennucci and E. Cances, *J. Mol. Struct.-Theo*, 1999, **464**, 211-
449 226.

450 42. F. M. Richards, *Ann. Rev. Biophys and Bioeng.*, 1977, **6**, 151-176.

451 43. L. Onsager, *J. Am. Chem. Soc.*, 1936, **58**, 1486-1493

452 44. F. Terenziani, A. Painelli, C. Katan, M. Charlot and M. Blanchard-Desce, *J. Am.*
453 *Chem. Soc.*, 2006, **128**, 15742-15755.

454 45. J. Cornil, I. Gueli, A. Dkhissi, J. C. Sancho-Garcia, E. Hennebicq, J. P. Calbert,
455 V. Lemaur, D. Beljonne and J. L. Bredas, *J. Chem. Phys.*, 2003, **118**, 6615-
456 6623.

457 46. X. L. Yue, Z. Armijo, K. King, M. V. Bondar, A. R. Morales, A. Frazer, I. A.
458 Mikhailov, O. V. Przhonska and K. D. Belfield, *ACS Appl. Mater. Interf.*, 2015,
459 **7**, 2833-2846.

460 47. M. G. Vivas, R. D. Fonseca, J. D. Siqueira, C. R. Mendonca, P. C. Rodrigues
461 and L. De Boni, *Materials*, 2017, **10**.

462 48. L. De Boni, R. D. Fonseca, K. R. A. Cardoso, I. Grova, L. Akcelrud, D. S.
463 Correa and C. R. Mendonca, *J. Polym. Sci. Part B-Polym. Phys.*, 2014, **52**, 747-
464 754.

465 49. D. S. Correa, L. De Boni, B. Nowacki, I. Grova, B. D. Fontes, P. C. Rodrigues,
466 J. R. Tozoni, L. Akcelrud and C. R. Mendonca, *J. Polym. Sci. Part B-Polym.*
467 *Phys.*, 2012, **50**, 148-153.

468 50. M. Daoud and M. Kibler, *Phys. Rev. B*, 1995, **52**, 12677-12680.

469 51. J. M. Hales, D. J. Hagan, E. W. Van Stryland, K. J. Schafer, A. R. Morales, K.
470 D. Belfield, P. Pacher, O. Kwon, E. Zojer and J. L. Bredas, *J. Chem. Phys.*,
471 2004, **121**, 3152-3160.

472 52. M. G. Vivas, L. De Boni and C. R. Mendonca, in *Molecular and Laser*
473 *Spectroscopy*, ed. V. P. Gupta, Elsevier 2018, vol. 1.

53. Y. C. Wang, S. H. Yin, J. Y. Liu, L. Yao, G. Q. Wang, D. J. Liu, B. Jing, L. H. Cheng, H. Y. Zhong, X. R. Shi, Q. Fang and S. X. Qian, *RSC Adv.*, 2014, **4**, 10960-10967.

54. K. D. Belfield, M. V. Bondar, A. R. Morales, X. L. Yue, G. Luchita and O. V. Przhonska, *J. Phys. Chem. C*, 2012, **116**, 11261-11271.

55. M. G. Vivas, D. L. Silva, L. De Boni, Y. Bretonniere, C. Andraud, F. Laibe-Darbour, J. C. Mulatier, R. Zalesny, W. Bartkowiak, S. Canuto and C. R. Mendonca, *J. Phys. Chem. Lett.*, 2013, **4**, 1753-1759.

56. G. Klaerner and R. D. Miller, *Macromol.*, 1998, **31**, 2007-2009.